22. Cohen, R., Erez, K., ben Avraham, D. & Havlin, S. Breakdown of the internet under intentional attack. *Phys. Rev. Lett.* **86,** 3682–3685 (2001).
23. Eubank, S., Anil Kumar, V., Marathe, M. V., Srinivasan, A. & Wang, N. in *Proc. ACM-SIAM Symp. Discrete Algorithms* (ed Munro, I.) 711–720 (SIAM Press, Philadelphia, 2004).
24. Dall, J. & Christensen, M. Random geometric graphs. *Phys. Rev. E* **66,** 016121 (2002).
25. Fenner, F., Henderson, D., Arita, I., Jezek, Z. & Ladnyi, I. *Smallpox and its Eradication* (World Health Organization, Geneva, 1988).
26. Eichner, M. & Dietz, K. Transmission potential of smallpox: estimates based on detailed data from an outbreak. *Am. J. Epidemiol.* **158,** 110–117 (2003).
27. Keeling, M. & Grenfell, B. T. Individual-based perspectives on R_0. *J. Theor. Biol.* **203,** 51–61 (2000).
28. Newman, M., Strogatz, S. & Watts, D. Properties of highly clustered networks. *Phys. Rev. E* **68,** 026121 (2003).

Supplementary Information accompanies the paper on **www.nature.com/nature.**

Acknowledgements We thank G. Korniss, G. Istrate and the Fogarty International Center at the National Institutes of Health for useful discussions, and acknowledge the work of all the members of the TRANSIMS and EpiSims team. The EpiSims project is funded by the National Infrastructure Simulation and Analysis Program (NISAC) at the Department of Homeland Security. The TRANSIMS project was funded by the Department of Transportation. H.G. was supported in part by the National Science Foundation (Division of Materials Research) and Z.T. by the Department of Energy. We thank the anonymous referees for their helpful suggestions.

Competing interests statement The authors declare that they have no competing financial interests.

Correspondence and requests for materials should be addressed to S.G.E. (eubank@lanl.gov).

Enhanced synaptic plasticity in newly generated granule cells of the adult hippocampus

Christoph Schmidt-Hieber, Peter Jonas & Josef Bischofberger

Physiologisches Institut der Universität Freiburg, D-79104 Freiburg, Germany

Neural stem cells in various regions of the vertebrate brain continuously generate neurons throughout life[1–4]. In the mammalian hippocampus, a region important for spatial and episodic memory[5,6], thousands of new granule cells are produced per day[7], with the exact number depending on environmental conditions and physical exercise[1,8]. The survival of these neurons is improved by learning and conversely learning may be promoted by neurogenesis[8–10]. Although it has been suggested that newly generated neurons may have specific properties to facilitate learning[2,10,11], the cellular and synaptic mechanisms of plasticity in these neurons are largely unknown. Here we show that young granule cells in the adult hippocampus differ substantially from mature granule cells in both active and passive membrane properties. In young neurons, T-type Ca^{2+} channels can generate isolated Ca^{2+} spikes and boost fast Na^+ action potentials, contributing to the induction of synaptic plasticity. Associative long-term potentiation can be induced more easily in young neurons than in mature neurons under identical conditions. Thus, newly generated neurons express unique mechanisms to facilitate synaptic plasticity, which may be important for the formation of new memories.

To identify newly generated granule cells in the adult hippocampus, we applied electrophysiological, morphological and immunocytochemical criteria. We made whole-cell recordings from neurons in the granule cell layer and determined the input resistance (R_{in}), which is known to be characteristically different between young and mature neurons[12]. Subsequently, we examined the immunoreactivity for polysialic acid neural cell adhesion molecule (PSA-NCAM), a marker for newly generated granule cells[1,3,13,14], and the morphology of the dendritic tree (Fig. 1).

On the basis of the distribution of R_{in}, most cells fell into two categories, with mean R_{in} values of 232 ± 78 MΩ and 4.5 ± 1.9 GΩ, respectively (mean ± s.d.; Fig. 1a, c, e). Cells with high R_{in} were exclusively encountered in the inner granule cell layer adjacent to the subgranular zone, where neural stem cells are located[1]. Cells with R_{in} below 400 MΩ were immunonegative for PSA-NCAM and showed a complex apical dendritic tree (total dendritic length 3,652 ± 134 μm; mean ± s.e.m.; $n = 14$), indicating that they were mature granule cells. In contrast, all cells with R_{in} larger than 1.5 GΩ were immunopositive for PSA-NCAM (Fig. 1d, f; relative fluorescence intensity 76 ± 6%) and had rudimentary apical and basal dendrites (Fig. 1f; total dendritic length 845 ± 111 μm, $n = 14$), indicative of immature granule cells[15–17]. As PSA-NCAM is expressed transiently in granule cells 1–3 weeks after mitosis[13,14], these results suggest that the cells with high R_{in} are newly generated immature granule cells in the adult hippocampus. Cells with R_{in} larger than 1.5 GΩ were immunonegative for parvalbumin ($n = 4$), suggesting that they do not represent interneurons[18,19].

We next studied the active and passive membrane properties of the two classes of neurons (Fig. 2). Both mature and young granule cells showed comparable resting potentials (−80.8 ± 0.9 mV versus −75.3 ± 2.0 mV, respectively) and were able to generate fast action potentials with large amplitudes (Fig. 2a–d; 140 ± 2 mV, $n = 9$ versus 115 ± 2 mV, $n = 6$). Unlike mature granule cells, which generated trains of action potentials during long current pulses (Fig. 2a; mean action potential frequency 30 ± 1 Hz), young neurons fired only a few action potentials per stimulus: in 15 of 20 cells, a single action potential was evoked (Fig. 2b). However, the current threshold determined with 100-ms pulses was markedly lower in young neurons than in mature cells (34 ± 9 pA, $n = 6$ versus 141 ± 12 pA, $n = 4$, respectively; $P < 0.01$). In a subset of young neurons currents of less than 10 pA were sufficient to elicit an action potential. Finally, young neurons had a much slower membrane time constant, τ_m, than mature granule cells (Fig. 2e, f; 123 ± 10 ms, $n = 7$ versus 54 ± 4 ms, $n = 13$, respectively)[20]. Thus, newly generated granule cells have membrane properties that favour action potential generation with very small current stimuli, such as the opening of less than ten glutamate receptor channels[21].

In contrast with mature neurons, young neurons generated transient low-threshold spikes when current injections below the threshold for Na^+ action potential initiation were applied (Figs 2b and 3). Low-threshold spikes were insensitive to 1 μM tetrodotoxin (TTX) but were blocked by 50 μM Ni^{2+}, showing that they were mediated by T-type Ca^{2+} channels[22] (Fig. 3a–c). Ca^{2+} spikes in newly generated neurons had a voltage threshold of −56.0 ± 1.2 mV and an amplitude of 17.6 ± 1.1 mV measured from the voltage at the end of the pulse ($n = 16$). Furthermore, they had a slow time course with a duration at half-maximal amplitude of 87 ± 8 ms ($n = 16$). Thus, young granule cells generate low-threshold Ca^{2+} spikes under physiological conditions, whereas mature granule cells produce low-threshold Ca^{2+} spikes only in the presence of K^+-channel blockers[23].

To examine whether the activation of T-type Ca^{2+} channels in young neurons contributed to the initiation of fast Na^+ action potentials, we determined the probability of Na^+ action potential initiation during current pulses of incremental amplitudes (Fig. 3d, e). A concentration of 50 μM Ni^{2+} markedly elevated the current threshold for the initiation of fast Na^+ action potentials (Fig. 3e). On average, the current corresponding to the mid-point of the threshold curves increased to 176 ± 56% of the control value in young neurons ($n = 6$, $P < 0.05$). By contrast, the threshold remained unchanged in mature neurons (98 ± 3%, $n = 4$). In conclusion, newly generated immature granule cells show a unique

pattern of excitability. As the stimulus intensity is increased, T-type Ca^{2+} channels first generate slow Ca^{2+} spikes and then boost the initiation of fast Na^{+} action potentials.

Postsynaptic action potentials are important associative signals for the induction of spike-timing-dependent plasticity at hippocampal glutamatergic synapses[24–26]. We therefore tested the impact of postsynaptic excitability on synaptic plasticity in young granule cells. Excitatory postsynaptic potentials (EPSPs) evoked by stimulation of the perforant path were examined in the perforated-patch configuration (Fig. 4). *In vivo* recordings suggest that dentate gyrus granule cells fire action potentials related to the location of the animal in the spatial environment and the phase of the hippocampal theta oscillation (5–8 Hz)[27,28]. To mimic this situation, we applied stimulation paradigms corresponding to the physiological firing pattern of a granule cell outside (TBS_0), at the border (TBS_1), or in the centre of its place field (TBS_2; Fig. 4a, see Methods). In mature granule cells, TBS_0 and TBS_1 failed to induce long-lasting changes in synaptic strength (Fig. 4b, d, f; the EPSP amplitudes 25–30 min after the end of the induction paradigm were 88 ± 13% ($n = 5$) and 92 ± 10% ($n = 6$) of the control value, respectively; $P > 0.4$). However, if bursts of postsynaptic action potentials were evoked during TBS_2, a long-term potentiation (LTP) of the EPSP amplitude was induced (214 ± 46% of control, $n = 6$, $P < 0.05$). Apparently, in mature granule cells a burst of postsynaptic action potentials was required for LTP induction, as reported previously for mature CA1 pyramidal neurons[25,29].

Similar to mature granule cells, TBS_0 failed to induce significant changes in EPSP amplitude in young granule cells (123 ± 19%,

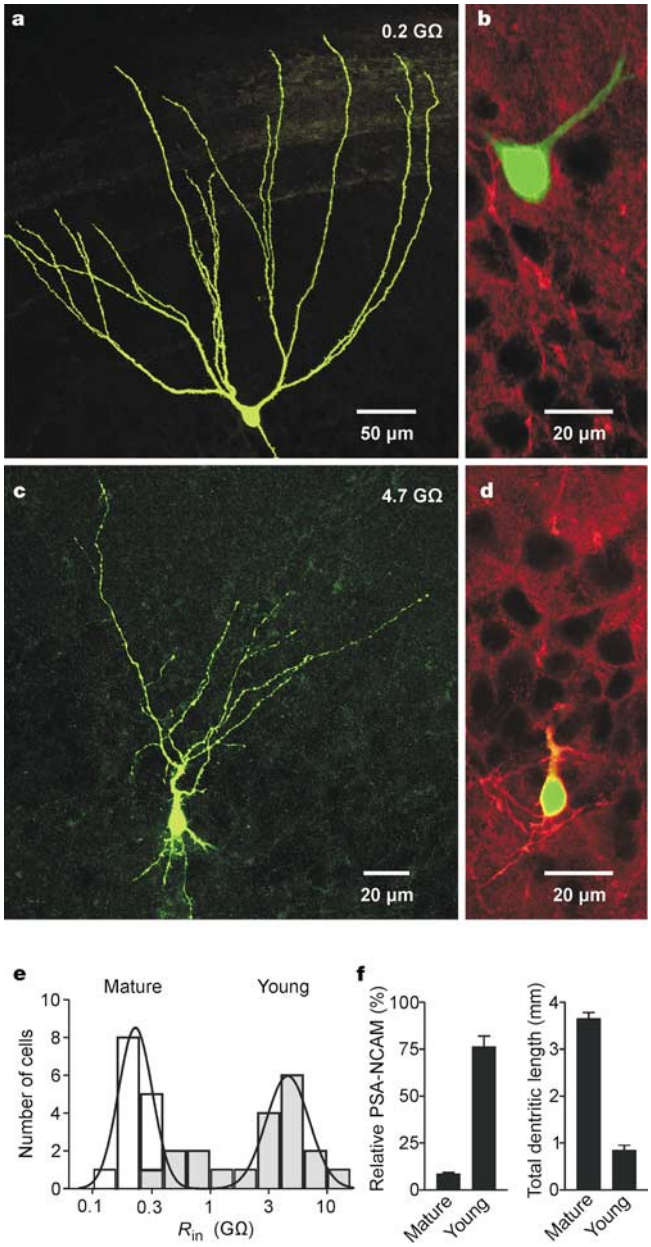

Figure 1 Newly generated granule cells in adult hippocampus are defined by high input resistance, PSA-NCAM immunoreactivity and immature dendritic morphology. **a**, **c**, Biocytin-filled mature (**a**) and young (**c**) granule cell. **b**, **d**, Confocal images of PSA-NCAM immunoreactivity (red) and biocytin staining (green) of the cells in **a** and **c**, respectively. Note the high PSA-NCAM expression of the immature cell (red dendrite and yellow rim at the soma). **e**, Distribution of input resistance of cells in the inner (grey bars) and outer part of the granule cell layer (open bars). Continuous curves represent the sum of two gaussian functions fitted to the histogram. **f**, Summary graph of PSA-NCAM immunoreactivity and total dendritic length.

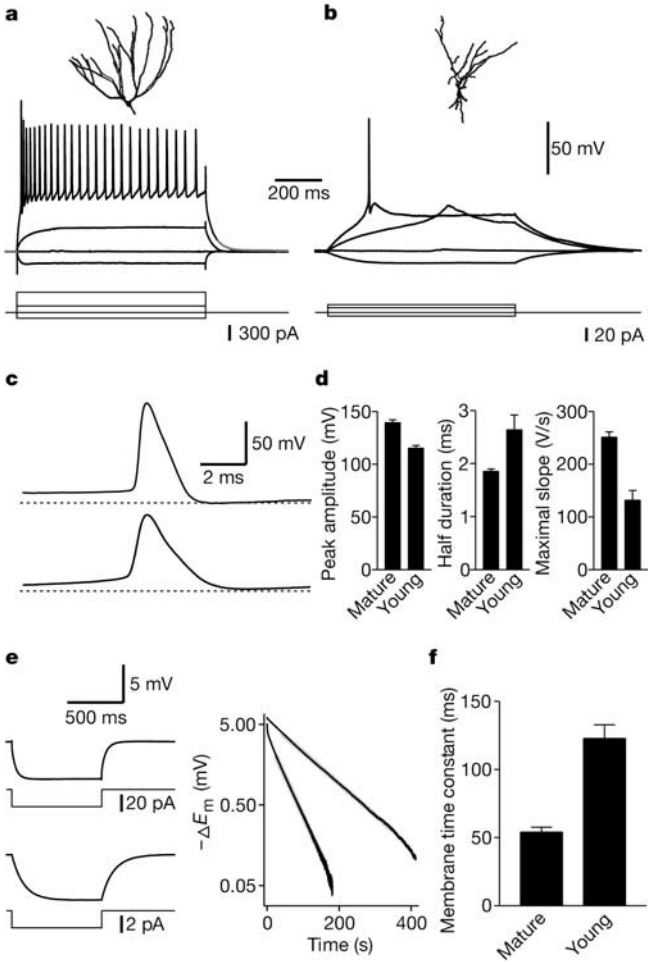

Figure 2 Young granule cells have distinct active and passive membrane properties. **a**, Train of action potentials in a mature neuron. **b**, Isolated low-threshold spike and single action potential in a young neuron. **c**, Single action potentials at higher time resolution in a mature (top trace) and a young neuron (bottom trace); dashed lines at −45 mV. **d**, Comparison of peak amplitude, half duration and maximal slope of action potentials. **e**, Voltage changes evoked by hyperpolarizing current pulses in a mature (top trace) and a young neuron (bottom trace). Right panel shows logarithmic plot of voltage changes (ΔE_m) after the pulse; regression lines (grey) are shown superimposed. **f**, Summary graph of membrane time constants.

$n = 5, P > 0.1$). However, unlike in mature cells TBS_1 was sufficient to induce LTP (Fig. 4c, e, g; the EPSP amplitude was 154 ± 9% of control, $n = 9, P < 0.01$). Furthermore, in the young cells TBS_2 had only slightly larger effects than TBS_1 (162 ± 10%, $n = 5$). Statistical comparison between young and mature cells further indicates that TBS_1 has significantly larger effects in the young neurons ($P < 0.001$). Thus, our results demonstrate that excitatory synapses on newly generated granule cells show associative plasticity, and that the threshold for induction is lower than in mature neurons. Pairing of EPSPs with single postsynaptic action potentials is a highly efficient stimulus for the induction of LTP in young granule cells, whereas a burst of postsynaptic action potentials is required in mature neurons. Hence, different induction rules for LTP apply to young and mature granule cells.

Newly generated granule cells show specialized membrane properties and enhanced associative plasticity at their glutamatergic input synapses, suggesting a causal link. One scenario is that the high input resistance and the expression of T-type Ca^{2+} channels promote LTP because they facilitate the activation of neurons by sparse glutamatergic synaptic inputs. Furthermore, Ca^{2+} and Na^{+} action potentials as evoked by TBS_1 in young granule cells may efficiently induce LTP by generating both a global rise in postsynaptic Ca^{2+} concentration and a maximal relief of Mg^{2+} block of NMDA-type glutamate receptors.

Functional plasticity such as TBS_1-induced LTP may have profound structural consequences. It is well established that PSA-NCAM selectively labels newly generated neurons 1–3 weeks after mitosis[13,14]. In this time period the fate of the newly generated neurons (survival versus cell death) is determined[30]. Enriched environment and spatial learning increase the proportion of surviving neurons[1,9], suggesting the possibility that associative LTP promotes the survival and final integration of newly generated granule cells into the adult hippocampal circuit.

Both functional and structural plasticity in newly generated cells may be important for the formation of spatial memory. Single spikes during the theta cycle are observed *in vivo* when the animal approaches the border of the place field of a hippocampal granule cell[27,28]. In the centre of the place field, however, granule cells fire brief bursts of action potentials. If the induction rules for synaptic plasticity as reported here also apply *in vivo*, our data would suggest that in young granule cells LTP will occur in a much larger 'induction area' as compared with mature neurons. This might be

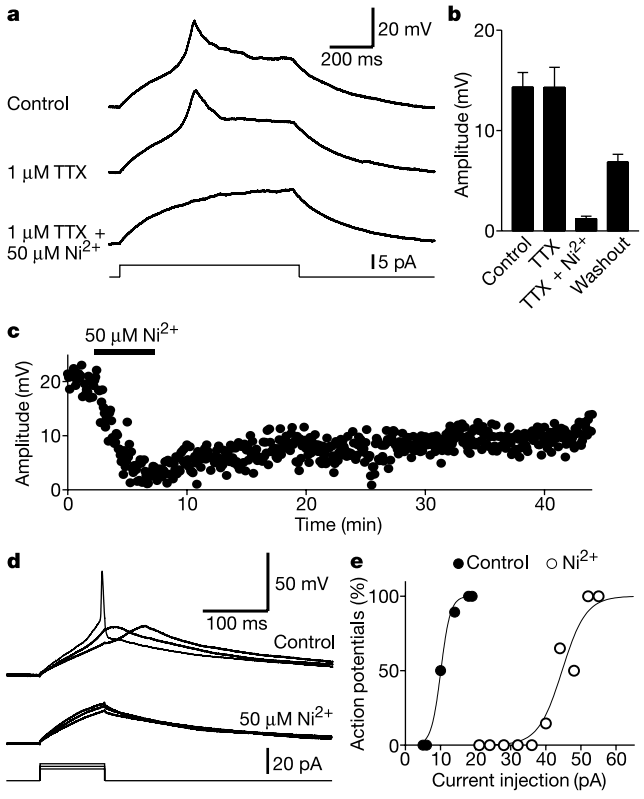

Figure 3 T-Type Ca^{2+} channels lead to enhanced excitability in young granule cells. **a**, **b**, The low-threshold spike in young neurons was insensitive to TTX, but was blocked by 50 μM Ni^{2+}, indicating that it is mediated by T-type Ca^{2+} channels. Spike amplitude was measured from the potential at the end of the current injection. **c**, Plot of Ca^{2+} spike amplitude against time in another experiment. The spike was reversibly blocked by Ni^{2+}. **d**, **e**, The current threshold for the initiation of Na^{+} action potentials was increased when T-type Ca^{2+} channels were blocked by Ni^{2+}. Continuous curves in **e** represent fitted Boltzmann functions.

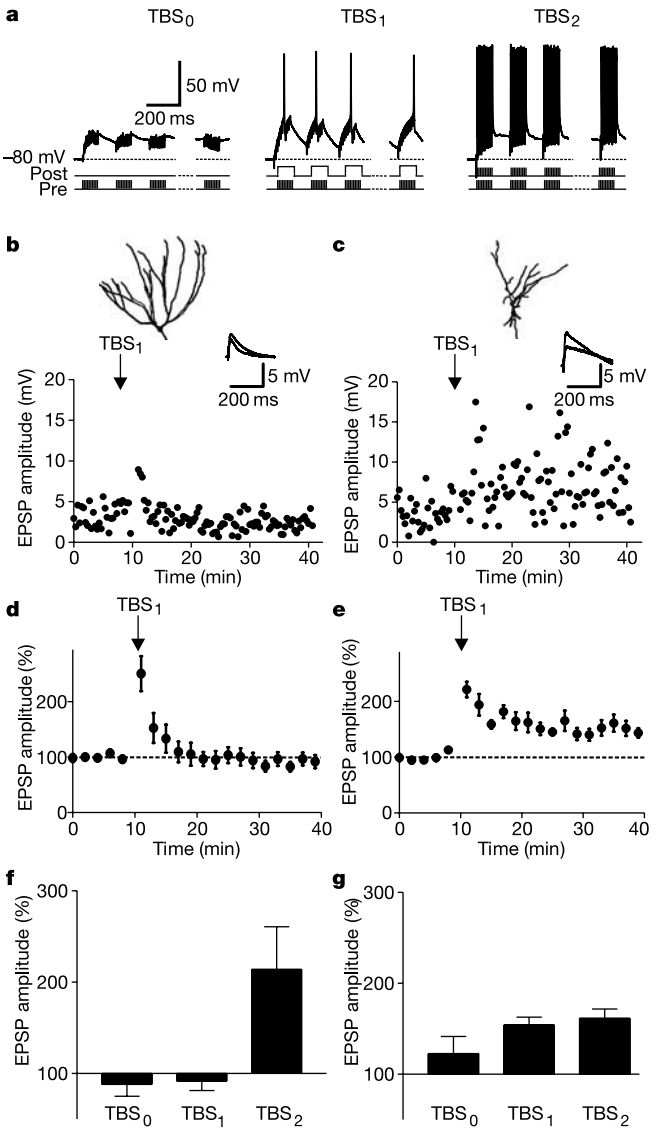

Figure 4 Different induction rules for long-term potentiation in young and mature neurons. **a**, Theta-burst induction paradigms, exemplified here for a young granule cell. **b**, **c**, Plot of EPSP amplitude against time in a mature (**b**) and a young (**c**) granule cell. **d**, **e**, Average plots for mature (**d**) and young (**e**) cells. In mature cells, TBS_1 had no effect, whereas it led to significant LTP in young cells. Data points represent means of six consecutive events. **f**, **g**, Summary of LTP experiments. TBS_1 led to LTP only in young neurons, whereas TBS_2 led to LTP in both mature and young cells. All data were from perforated-patch recordings.

important for the formation of new place fields. As the dendritic tree grows and the cell becomes fully integrated into the hippocampal circuit, a burst of action potentials will be necessary for LTP induction. Thus, the induction area will be much more confined, finally leading to a high spatial selectivity and a precise neuronal encoding of new spatial environment[6]. □

Methods

Slice preparation

Adult male Wistar rats (2–3 months old, approximately 300 g) were reared in large cages with running wheels and climbing frames. The animals were anaesthetized by isoflurane and killed by decapitation, in accordance with institutional guidelines. Transverse 350-μm-thick slices were cut from the hippocampus using a vibratome (DTK-1000; Dosaka). For the dissection and the storage of the slices, a solution containing 64 mM NaCl, 25 mM $NaHCO_3$, 10 mM glucose, 120 mM sucrose, 2.5 mM KCl, 1.25 mM NaH_2PO_4, 0.5 mM $CaCl_2$ and 7 mM $MgCl_2$ (equilibrated with 95% O_2/5% CO_2) was used. Slices were incubated at 35 °C for 30 min and subsequently held at room temperature.

Immunohistochemistry and morphology

Cells were filled with biocytin (1 mg ml^{-1}) during whole-cell recording and subsequently fixed in 4% paraformaldehyde. After washing, tissue sections were incubated overnight at 4 °C with the primary antibody for PSA-NCAM (mouse, Chemicon, 1:400) together with 5% goat serum and 0.3% Triton X-100. The secondary antibody (goat anti-mouse-Alexa546, 1:200, Molecular Probes) was applied together with fluorescein isothiocyanate-conjugated avidin-D (2 μl ml^{-1}, Vector) and 0.3% Triton X-100 for 24 h at 4 °C. After washing, slices were embedded in Prolong Antifade (Molecular Probes). Parvalbumin immunoreactivity was tested using an antibody against parvalbumin (mouse, Swant, 1:5,000) and an Alexa568-conjugated secondary antibody. Fluorescence was analysed with a confocal laser-scanning microscope (LSM 510, Zeiss).

PSA-NCAM immunofluorescence was measured in 1-μm optical sections and quantified as intensity per pixel along the somatic cell membrane. Background intensity was subtracted, and the signal was normalized by the mean intensity of the brightest 1% of pixels within the image (325 × 325 μm). The morphology of the cells was reconstructed in three dimensions from a stack of 50–100 confocal images using NeuronTracer software (Bitplane) running on an O2 workstation (Silicon Graphics). The total dendritic length was calculated as the sum of the lengths of all dendritic segments. Only cells with intact dendrites were used.

Electrophysiology

Slices were superfused with a physiological extracellular solution containing 125 mM NaCl, 25 mM $NaHCO_3$, 25 mM glucose, 2.5 mM KCl, 1.25 mM NaH_2PO_4, 2 mM $CaCl_2$ and 1 mM $MgCl_2$ (equilibrated with 95% O_2/5% CO_2). A concentration of 10 μM bicuculline methiodide was added in plasticity experiments, and 10 μM bicuculline and 10 μM 6-cyano-7-nitroquinoxaline-2,3-dione (CNQX) in membrane time constant experiments. Recordings were performed under visual control. Patch pipettes (4–9 MΩ) were pulled from thick-walled borosilicate glass tubing. Voltage signals were measured with an Axopatch 200A amplifier (Axon Instruments) in the I-clamp fast mode, filtered at 5 kHz, and digitized at 10 or 20 kHz using a 1401plus interface (Cambridge Electronic Design). For whole-cell recordings, pipettes were filled with a solution containing 130 mM K-gluconate, 20 mM KCl, 2 mM $MgCl_2$, 4 mM K_2ATP, 0.3 mM NaGTP, 10 mM Na_2-phosphocreatine and 10 mM HEPES (pH 7.2). For perforated-patch recordings, a pipette solution containing 140 mM K-gluconate, 20 mM KCl, 5 mM $MgCl_2$, 10 mM HEPES, 0.1 mM EGTA, 50–100 μg ml^{-1} amphotericin B and 0.2–0.4% DMSO was used. Bridge balance was used to compensate the series resistance of 10–50 MΩ (whole cell) or 60–90 MΩ (perforated patch). Resting potential was determined in a subset of recordings with seal resistances $>5R_{in}$. The holding potential was set to −80 mV. To stimulate the medial perforant path, 2–4-MΩ pipettes filled with HEPES-buffered Na^+-rich solution were used. The pipettes were placed in the centre of the molecular layer close to the dendrites of the recorded cell, and 200-μs pulses were applied at a frequency of 0.05 Hz. EPSP amplitude measurements were started 10–15 min after a stable access resistance had developed. Recordings were performed at 21–23 °C.

LTP induction protocols

The LTP induction paradigms consisted of brief presynaptic bursts (ten stimuli at 100 Hz) repeated ten times at theta frequency (5 Hz). This presynaptic stimulation was applied alone (TBS_0), paired with a slow postsynaptic depolarization that typically evoked a single action potential (TBS_1), or paired with a train of brief stimuli that evoked a burst of postsynaptic action potentials[25,29] (TBS_2; 5-ms delay between pre- and postsynaptic train). Paradigms were applied four times at 0.1 Hz. Only one TBS paradigm was tested per cell. If no LTP occurred, a maximal high-frequency stimulation protocol was applied (100 Hz, 1 s, four times, paired to postsynaptic depolarizations to 0 mV), and experiments were rejected if no LTP could be induced (8 of 24 mature and 4 of 23 young cells).

Data analysis

The input resistance was determined from the voltage at the end of 500- or 800-ms current pulses leading to approximately 5 mV hyperpolarization. To determine the membrane time constant, 200–400 voltage traces were averaged, and the logarithmically transformed decay was analysed by linear regression. For the quantification of LTP, 15 or 30 consecutive EPSPs were averaged 10 min before the onset and 25–30 min after the end of the induction protocol. Peak amplitudes were measured from holding potential and data are given as mean ± s.e.m. unless specified differently. A Wilcoxon signed rank test or a Mann–Whitney test were used to assess statistical significance.

Received 2 February; accepted 8 April 2004; doi:10.1038/nature02553.
Published online 25 April 2004.

1. Gage, F. H. Mammalian neural stem cells. *Science* **287,** 1433–1438 (2000).
2. Nottebohm, F. Why are some neurons replaced in adult brain? *J. Neurosci.* **22,** 624–628 (2002).
3. Seki, T. & Arai, Y. Highly polysialylated neural cell adhesion molecule (NCAM-H) is expressed by newly generated granule cells in the dentate gyrus of the adult rat. *J. Neurosci.* **13,** 2351–2358 (1993).
4. van Praag, H. *et al.* Functional neurogenesis in the adult hippocampus. *Nature* **415,** 1030–1034 (2002).
5. Lisman, J. E. Relating hippocampal circuitry to function: recall of memory sequences by reciprocal dentate-CA3 interactions. *Neuron* **22,** 233–242 (1999).
6. Burgess, N., Maguire, E. A. & O'Keefe, J. The human hippocampus and spatial and episodic memory. *Neuron* **35,** 625–641 (2002).
7. Cameron, H. A. & McKay, R. D. G. Adult neurogenesis produces a large pool of new granule cells in the dentate gyrus. *J. Comp. Neurol.* **435,** 406–417 (2001).
8. van Praag, H., Christie, B. R., Sejnowski, T. J. & Gage, F. H. Running enhances neurogenesis, learning, and long-term potentiation in mice. *Proc. Natl Acad. Sci. USA* **96,** 13427–13431 (1999).
9. Gould, E., Beylin, A., Tanapat, P., Reeves, A. & Shors, T. J. Learning enhances adult neurogenesis in the hippocampal formation. *Nature Neurosci.* **2,** 260–265 (1999).
10. Shors, T. J. *et al.* Neurogenesis in the adult is involved in the formation of trace memories. *Nature* **410,** 372–376 (2001).
11. Snyder, J. S., Kee, N. & Wojtowicz, J. M. Effects of adult neurogenesis on synaptic plasticity in the rat dentate gyrus. *J. Neurophysiol.* **85,** 2423–2431 (2001).
12. Liu, Y.-B., Lio, P. A., Pasternak, J. F. & Trommer, B. L. Developmental changes in membrane properties and postsynaptic currents of granule cells in rat dentate gyrus. *J. Neurophysiol.* **76,** 1074–1088 (1996).
13. Seki, T. Hippocampal adult neurogenesis occurs in a microenvironment provided by PSA-NCAM-expressing immature neurons. *J. Neurosci. Res.* **69,** 772–783 (2002).
14. Seki, T. Expression patterns of immature neuronal markers PSA-NCAM, CRMP-4 and NeuroD in the hippocampus of young adult and aged rodents. *J. Neurosci. Res.* **70,** 327–334 (2002).
15. Lübbers, K. & Frotscher, M. Differentiation of granule cells in relation to GABAergic neurons in the rat fascia dentata. Combined Golgi/EM and immunocytochemical studies. *Anat. Embryol.* **178,** 119–127 (1988).
16. Rihn, L. L. & Claiborne, B. J. Dendritic growth and regression in rat dentate granule cells during late postnatal development. *Dev. Brain Res.* **54,** 115–124 (1990).
17. Rao, M. S. & Shetty, A. K. Efficacy of doublecortin as a marker to analyse the absolute number and dendritic growth of newly generated neurons in the adult dentate gyrus. *Eur. J. Neurosci.* **19,** 234–246 (2004).
18. Jonas, P., Bischofberger, J., Fricker, D. & Miles, R. Interneuron diversity series: Fast in, fast out—temporal and spatial signal processing in hippocampal interneurons. *Trends Neurosci.* **27,** 30–40 (2004).
19. Liu, S. *et al.* Generation of functional inhibitory neurons in the adult rat hippocampus. *J. Neurosci.* **23,** 732–736 (2003).
20. Spruston, N. & Johnston, D. Perforated patch-clamp analysis of the passive membrane properties of three classes of hippocampal neurons. *J. Neurophysiol.* **67,** 508–529 (1992).
21. Spruston, N., Jonas, P. & Sakmann, B. Dendritic glutamate receptor channels in rat hippocampal CA3 and CA1 pyramidal neurons. *J. Physiol. (Lond.)* **482,** 325–352 (1995).
22. Eliot, L. S. & Johnston, D. Multiple components of calcium current in acutely dissociated dentate gyrus granule neurons. *J. Neurophysiol.* **72,** 762–777 (1994).
23. Blaxter, T. J., Carlen, P. L. & Niesen, C. Pharmacological and anatomical separation of calcium currents in rat dentate granule neurones *in vitro*. *J. Physiol. (Lond.)* **412,** 93–112 (1989).
24. Debanne, D., Gähwiler, B. H. & Thompson, S. M. Cooperative interactions in the induction of long-term potentiation and depression of synaptic excitation between hippocampal CA3–CA1 cell pairs *in vitro*. *Proc. Natl Acad. Sci. USA* **93,** 11225–11230 (1996).
25. Magee, J. C. & Johnston, D. A synaptically controlled, associative signal for Hebbian plasticity in hippocampal neurons. *Science* **275,** 209–213 (1997).
26. Normann, C. *et al.* Associative long-term depression in the hippocampus is dependent on postsynaptic N-type Ca^{2+} channels. *J. Neurosci.* **20,** 8290–8297 (2000).
27. Jung, M. W. & McNaughton, B. L. Spatial selectivity of unit activity in the hippocampal granular layer. *Hippocampus* **3,** 165–182 (1993).
28. Skaggs, W. E., McNaughton, B. L., Wilson, M. A. & Barnes, C. A. Theta phase precession in hippocampal neuronal populations and the compression of temporal sequences. *Hippocampus* **6,** 149–172 (1996).
29. Pike, F. G., Meredith, R. M., Olding, A. W. A. & Paulsen, O. Postsynaptic bursting is essential for 'Hebbian' induction of associative long-term potentiation at excitatory synapses in rat hippocampus. *J. Physiol. (Lond.)* **518,** 571–576 (1999).
30. Dayer, A. G., Ford, A. A., Cleaver, K. M., Yassaee, M. & Cameron, H. A. Short-term and long-term survival of new neurons in the rat dentate gyrus. *J. Comp. Neurol.* **460,** 563–572 (2003).

Acknowledgements We thank M. Frotscher, E. Förster and G. Stuart for critically reading the manuscript, and K. Winterhalter and A. Blomenkamp for technical assistance. Work was supported by the Deutsche Forschungsgemeinschaft.

Competing interests statement The authors declare that they have no competing financial interests.

Correspondence and requests for materials should be addressed to J.B. (josef.bischofberger@uni-freiburg.de).